Decentralized Droop Control in DC Microgrids Based on a Frequency Injection Approach

Peyghami, Saeed; Davari, Pooya; Mokhtari, Hossein; Blaabjerg, Frede

Published in:
I E E E Transactions on Smart Grid

DOI (link to publication from Publisher):
10.1109/TSG.2019.2911213

Publication date:
2019

Document Version
Accepted author manuscript, peer reviewed version

Decentralized Droop Control in DC Microgrids Based on a Frequency Injection Approach

Saeed Peyghami[1], *Member IEEE*, Pooya Davari[1], *Senior Member IEEE*,
Hossein Mokhtari[2], *Senior Member IEEE*, and Frede Blaabjerg[1], *Fellow IEEE*

***Abstract*—Power sharing control among grid forming DC sources employing a conventional voltage droop approach meets inaccurate load sharing and unacceptable voltage regulation performance. Thereby, communication-based secondary and supervisory controllers have been presented to overcome the aforementioned issues. Furthermore, with the aim of eliminating communication system, frequency-based droop approaches have been introduced for low voltage DC grids where the frequency of the superimposed AC signal onto the DC voltage is proportional to the output power. However, in reality, DC grid structures can be applied to medium and high voltage applications with different X/R ratios. This paper generalizes the frequency-based droop scheme for DC microgrids with different low, medium and high *X/R* ratios. Obtained simulation and experiment results demonstrate the effectiveness of the proposed control method.**

***Index Terms*— DC grid, droop control, frequency droop, grid forming, power sharing.**

I. INTRODUCTION

With the recent advances in power electronic converters DC power systems are gaining more interest over AC systems from generation, transmission down to distribution levels [1]–[4]. In fact, DC power systems can introduce higher efficiency, reliability and power quality than their AC system counterparts. Furthermore, availability of a DC link in the corresponding power conversion stages of most of loads and sources shows the feasibility of implementing DC power systems.

DC grid structures have a wide range of applications from low to high voltages as shown in Fig. 1. Energy resources in DC systems can be classified as non-dispatchable units like Photo-Voltaic (PV) arrays and Wind Turbines (WT), and dispatchable units like battery storages, Fuel Cell (FC) modules, micro-turbines, and hybrid battery-PV [5]. Non-dispatchable units always operate as a current source, and thus, they are not controllable sources. The reference power of dispatchable units are economically determined by energy management system considering the forecasted load and renewable energy-based units as well as operational costs and emissions during planning. However, during the operation, power sharing control approaches are required to balance the generation-demand, regulate the grid voltage, and prevent overstressing of the converters. Hence, dispatchable units require to be controlled by a suitable load/power sharing method [6], [7]. Conventional voltage-based droop methods are employed to control the loading of the converters by utilizing a virtual resistor [6], [8]–[12]. However, in the conventional virtual resistor-based droop method, as the voltage is a local variable, its performance is highly dependent on the virtual resistor value, which can either results in a poor accuracy or instability.

In order to solve the aforementioned challenges, modified load/power sharing methods have been presented in DC grids [7], [10], [13]. In [10] load sharing and voltage regulation accuracy are enhanced by regulating the average values of per-unit current and voltage of sources in the secondary and/or supervisory control layer. This approach requires a full communication network among the DC sources. Moreover, utilizing the information of neighboring sources (i.e., voltage and current) can results in obtaining better power sharing and voltage regulation accuracy based on a dynamic consensus protocol [7]. This method is similar to the circular current chain (CCC) approach employed for power sharing control among parallel-connected Uninterruptable Power Supply (UPS) units [14], [15]. However, implementing the secondary controllers based on sharing voltage and current information through communication system may impair the system stability and reliability [7].

Taking into account the above discussion, few decentralized approaches are presented based on network-less communication. A voltage droop method with non-linear characteristics is introduced in [16], which not only reduces the effect of virtual resistor on voltage drops, but also improves the load sharing accuracy. In [17], frequency encoding of converter's output currents has been employed to implement a power sharing method. A power sharing scheme based on frequency droop approach is proposed for Low Voltage DC (LVDC) microgrids in [18], where it was confronted with main issues including frequency selection, DC voltage and AC power coupling analysis and DC voltage regulation. These issues are fully investigated in [19], [20] and the feasibility of the method is validated for low voltage DC microgrids.

However, the DC grid technology is also widely employed in Medium Voltage (MV) and High Voltage (HV) levels. The electrical network of ship-boards, off-shore oil-drilling units, PV parks, wind farms, and distribution systems is based on the MVDC technology [2], [21]–[26]. For example, an MVDC distribution system is shown in Fig. 1(a) inter-connecting different energy units and loads. Moreover, an electric network of a ship-board with MVDC distribution system is shown in Fig. 1(b).

This work was supported by VILLUM FONDEN under the VILLUM Investigators Grant called REPEPS.

[1] S. Peyghami, P. Davari, and F. Blaabjerg are with the Department of Energy Technology, Aalborg University, Denmark (sap@et.aau.dk).

[2] H. Mokhtari is with the Department of Electrical Engineering, Sharif University of Technology, Iran.

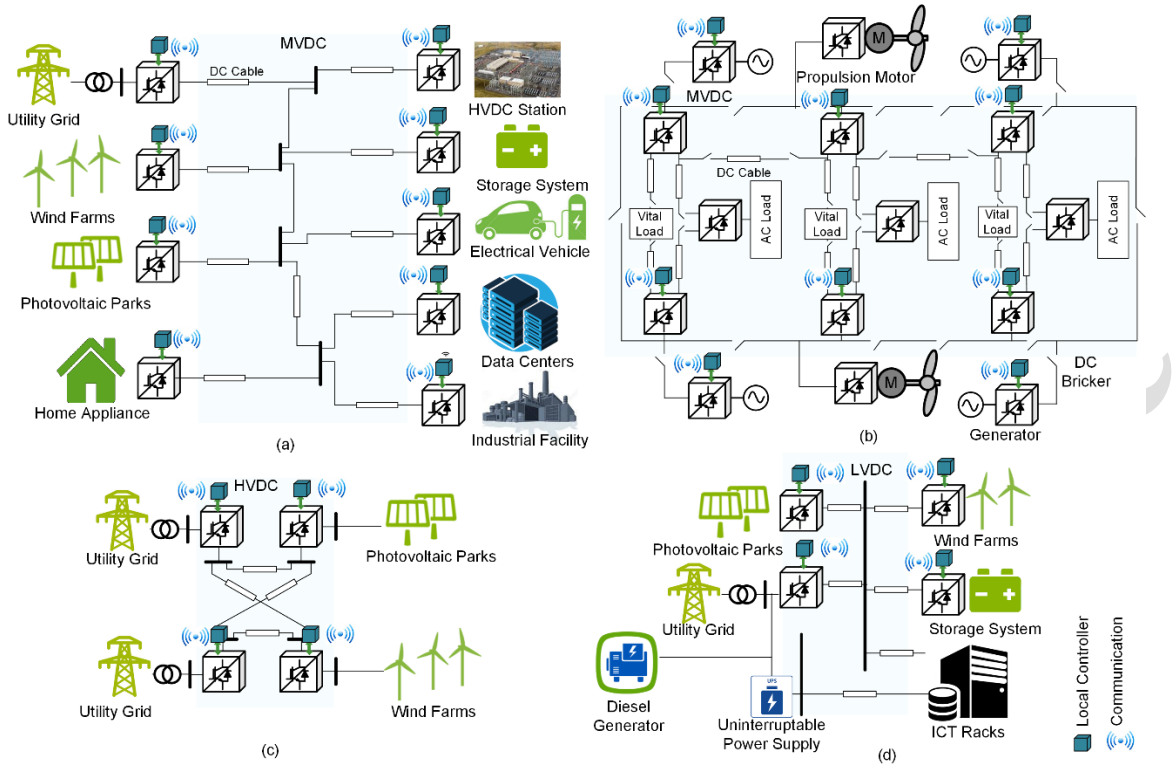

Fig. 1. DC grid architectures for (a) MVDC Distribution systems and (b) MVDC electric ship-boards, (c) HVDC transmission system, (d) LVDC data center.

Furthermore, Ultra High/ High Voltage Direct Current (UH/HVDC) transmission systems (from 300 kV to 800 kV) are playing key-role in connecting remote generations, interconnecting AC grids, connecting off-shore wind farms to the grids [21], [25], [27]. For instance, Fig. 1(c) shows a four-terminal HVDC system connecting large-scaled PV park and wind farm to the two AC grids. LVDC grid architectures are also employed in space-crafts, space stations, data centers, low voltage distribution systems, photovoltaic parks and etc. in different voltage range of 24 V to 1 kV [20], [28]–[32]. Fig. 1(d) illustrated an LVDC grid architecture for data center application.

In such applications, the voltage level varies from a few volts to hundred kilo-volts, implying different *X/R* ratios of lines [33]. This fact will affect the performance of the frequency droop controller, where the frequency is proportional to the reactive power in low *X/R* ratio grids. However, employing the frequency-based droop approach for high and medium voltage DC power systems with different *X/R* ratios requires suitable adjustment of the frequency-droop control structure.

This paper provides theoretical analysis to show the relation between *X/R* ratio and frequency-based droop control. Afterwards, the DC to AC coupling is modified by a virtual resistor for medium *X/R* ratio systems. Furthermore, active power is used as a coupling power between AC and DC signals in the case of high *X/R* ratio. As a consequence, the power sharing among different sources in medium and high voltage systems can be carried out without employing extra communication network. This fact will improve the overall reliability by eliminating the communication system especially in the applications with long distances. Moreover, this paper introduces an event-trigged frequency droop control for DC systems to further improve the performance of the control strategy presented in [19], [20]. In the even-triggered approach, a limiting-time AC signal injection will enhance the power quality, efficiency and reliability of the overall system.

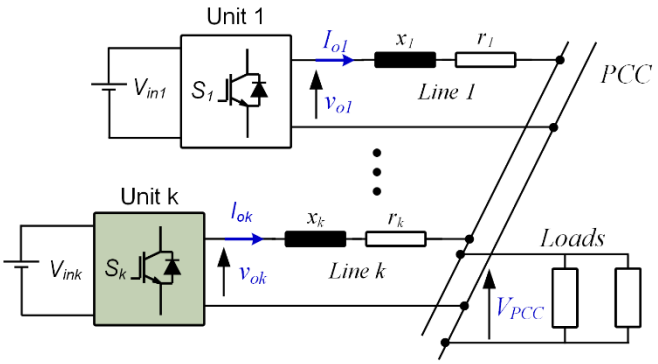

Fig. 2. Block diagram of a DC grid architecture with DC-DC converters as sources – PCC: Point of Common Coupling

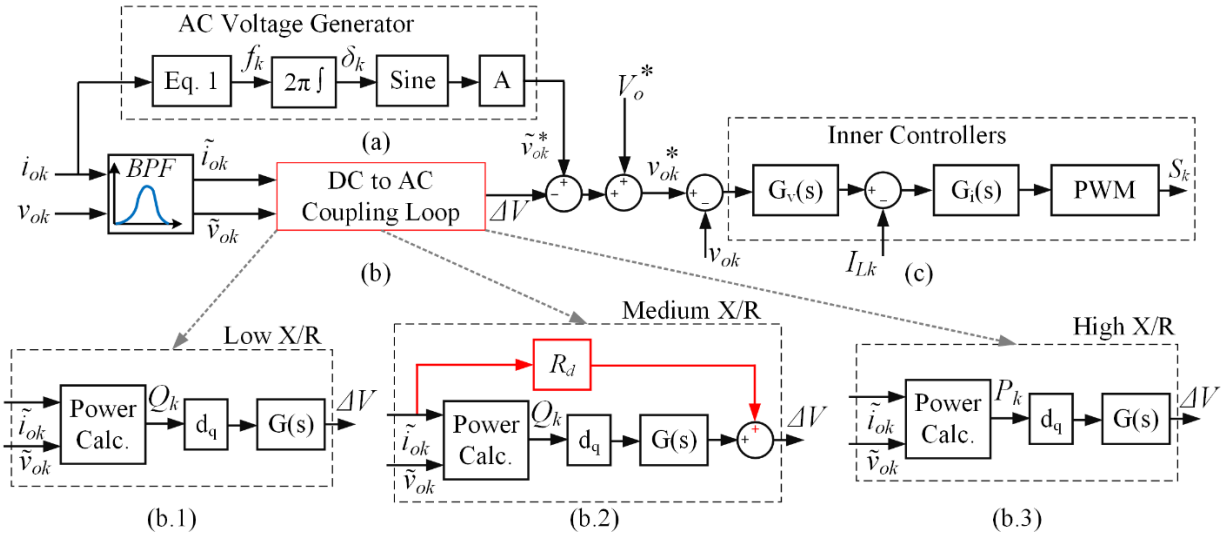

Fig. 3. Block diagram of frequency droop approach in DC grids for k^{th} converter: (a) AC voltage generator based on frequency droop, (b) DC voltage and AC power coupling loop configurable for: (b.1) low X/R, (b.2) medium X/R and (b.3) high X/R ratios ($G(s)$ is a first order low pass filter with cut-off frequency of ω_c), and (c) control loops block diagram (with $G_v(s)$ and $G_i(s)$ as voltage and current controllers).

Therefore, this paper provides further analysis and generalizes the frequency droop strategy presented in [19], [20] as a decentralized power sharing approach for high/medium/low *X/R* ratio of DC grids. The basics of the frequency-based droop method and proposed droop approach are explained in Section II. Sections III and IV are dedicated to the obtained simulation and experimental results to demonstrate the effectiveness of the control approach. Moreover, Section V presents the future perspective of the proposed approach by stopping the signal injection during steady state condition. Section VI further evaluates the viability of the control strategy with unequal load sharing. Finally, conclusions are drawn in Section VII.

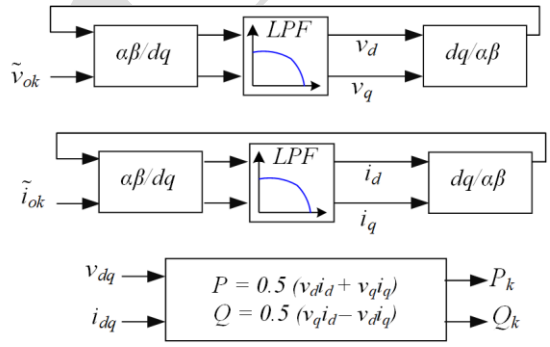

Fig. 4. Power Calculation block in Fig. 3.

II. Proposed Frequency Droop Control

The main idea of the frequency-based droop method in DC grids is to superimpose an AC voltage to the DC voltage by the grid forming sources. Thereby, the DC sources will be operating like synchronous generators working in droop method. The next subsection explains the concept of frequency droop control according to [19], [20].

A. Droop Control Approach

Fig. 2 shows a DC grid with DC-DC converters supplying the distributed loads. The proposed control structure of the k^{th} converter is shown in Fig. 3 and the power calculation block is shown in Fig. 4. Following Fig. 3(a), DC sources can generate an AC voltage $\tilde{v}_{ok}$ with a constant amplitude, e.g., 0.6% (denoted as *A*) and a frequency f_k as shown in Fig. 5.

The superimposed frequency is proportional to the converter current i_{ok} as [19]:

$$f_k = f^* - d_{fk} i_{ok} \ , \tag{1}$$

where f^* is the nominal frequency, and d_{fk} is the k^{th} converter's droop gain. Since the inner voltage/current regulators (see Fig. 3(c)) generate the superimposed AC voltage, the injected frequency will be limited by the bandwidth of the voltage controller

Following frequency droop method principle, the frequency of the converters will reach a common steady state value, resulting in proportional load sharing among the converters. Consequently, the superimposed frequency can be employed to make coordination among the converters. Therefore, the converters can properly operate by employing local voltage and current values without using any communication among them. Notably, they are synchronized based on the droop theory like the parallel operated synchronous generators in conventional power systems as well as droop controlled converters in ac microgrids [19], [33].

The output current of converters is controlled by DC voltages as:

$$I_{ok} = \frac{V_{ok} - V_{PCC}}{r_k} \tag{2}$$

where I_{ok} and V_{ok} are the output current and voltage of k^{th} converter, r_k being the k^{th} line resistance, and V_{PCC} is the voltage at the Point of Common Coupling (PCC). In order to

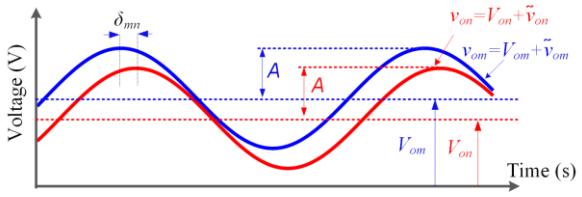

Fig. 5. Conceptualize illustration of the proposed frequency injection method.

make a coupling between AC and DC signals, the DC voltages require to be controlled by an AC parameter, denoted as Coupling Power (*CP*), which should be proportional to the injected AC voltage frequency. Thereby, the DC voltage is affected by the frequency, which is associated with the DC current as given in (1). Meanwhile, the DC current of converters are controlled by the corresponding DC voltages as given in (2). Consequently, the coupling between AC and DC signals can be properly defined if a suitable parameter *CP* is found. According to Fig. 3(a) and (1), the phase of the superimposed AC voltage for unit *k*, (δ_k) can be expressed as:

$$\delta_k(t) = 2\pi\int_0^t \left(f^* - d_{fk} i_{ok}(\tau) \right) d\tau \tag{3}$$

Following Fig. 5, the relative phase (δ_{mn}) between the AC voltages of the m^{th} and n^{th} converters is thus equal to:

$$\delta_{mn}(t) = \delta_m(t) - \delta_n(t) = 2\pi\int_0^t \left(d_{fn} i_{on}(\tau) - d_{fm} i_{om}(\tau) \right) d\tau \tag{4}$$

If current sharing between units *m* and *n* is not carried out based on the corresponding droop gains, following (4), δ_{mn} will not be zero. If the load has higher impedance that the line, a small AC power will flow between the converters [19], [20].

The reactive power is used in [19], [20] as an AC power coupling for low voltage DC grids since the frequency is associated with the reactive power in low voltage systems [15].

Therefore, the frequency-based droop control can be accomplished as shown in Fig. 3(b.1). Coupling the DC voltage to the injected reactive power (*CP* = *Q*) as (5) results in an accurate current sharing.

$$\begin{aligned} V_{ok} &= V_o^* - \Delta V \\ \Delta V &= d_q Q_k \end{aligned}, \tag{5}$$

in which V_o^* and V_{ok} are the reference values and output DC voltage of the k^{th} converter and d_q is the coupling coefficient of reactive power to the DC voltage.

However, for the DC systems with different *X/R* ratios, another coupling parameter should be employed. In order to find a suitable coupling parameter, the impact of line impedance on the current sharing is explained in the following.

B. Analysis of Line Impedance Effects

Fig. 6 shows the AC equivalent circuit of a simplified DC grid with two DC-DC converters. Two sources are connected to a resistive load at the PCC. The "Δ" equivalent model of this network is shown in Fig. 6(b). Considering the AC voltage

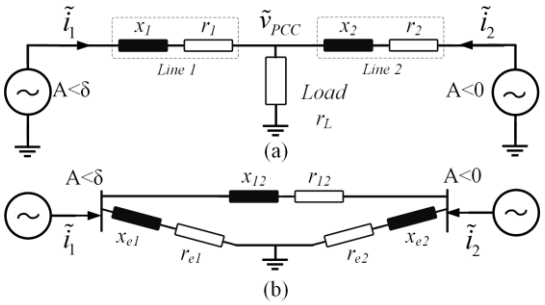

Fig. 6. AC equivalent circuit representation of a DC grid based on two sources, (a) actual connections, (b) Δ equivalent circuit of (a).

magnitudes to be equal to (*A*) and relative phase angle equal to (δ), the injected AC powers of both converters can be calculated as (6)–(9).

$$P_1 = \frac{r_{e1}}{2\left(r_{e1}^2 + x_{e1}^2\right)} A^2 + \frac{A^2}{\sqrt{r_{12}^{\,2} + x_{12}^{\,2}}} \sin\left(\phi + \frac{\delta}{2}\right) \sin\left(\frac{\delta}{2}\right) \tag{6}$$

$$Q_1 = \frac{x_{e1}}{2\left(r_{e1}^2 + x_{e1}^2\right)} A^2 - \frac{A^2}{\sqrt{r_{12}^{\,2} + x_{12}^{\,2}}} \cos\left(\phi + \frac{\delta}{2}\right) \sin\left(\frac{\delta}{2}\right) \tag{7}$$

$$P_2 = \frac{r_{e2}}{2\left(r_{e2}^2 + x_{e2}^2\right)} A^2 - \frac{A^2}{\sqrt{r_{12}^{\,2} + x_{12}^{\,2}}} \sin\left(\phi - \frac{\delta}{2}\right) \sin\left(\frac{\delta}{2}\right) \tag{8}$$

$$Q_2 = \frac{x_{e2}}{2\left(r_{e2}^2 + x_{e2}^2\right)} A^2 + \frac{A^2}{\sqrt{r_{12}^{\,2} + x_{12}^{\,2}}} \cos\left(\phi - \frac{\delta}{2}\right) \sin\left(\frac{\delta}{2}\right) \tag{9}$$

where P_k and Q_k are the active and reactive power injected by the k^{th} converter. Line impedances are illustrated in the Fig. 6 with (r_1, x_1) and (r_2, x_2) being the impedance of line 1 and 2 respectively, r_L as the load resistance, (r_{12}, x_{12}) as the impedance of equivalent line between the two converters and Φ being the phase angle of this impedance. (r_{e1}, x_{e1}) and (r_{e2}, x_{e2}) are the parallel equivalent impedances of the circuit. Considering $r_L >> (r_1, r_2)$, the first part of AC powers can be neglected. Hence, the injected AC powers by both converters can be rewritten as (10)–(13).

$$P_1 \approx +\frac{A^2}{\sqrt{r_{12}^{\,2} + x_{12}^{\,2}}} \sin\left(\phi + \frac{\delta}{2}\right) \sin\left(\frac{\delta}{2}\right) \tag{10}$$

$$Q_1 \approx -\frac{A^2}{\sqrt{r_{12}^{\,2} + x_{12}^{\,2}}} \cos\left(\phi + \frac{\delta}{2}\right) \sin\left(\frac{\delta}{2}\right) \tag{11}$$

$$P_2 \approx -\frac{A^2}{\sqrt{r_{12}^{\,2} + x_{12}^{\,2}}} \sin\left(\phi - \frac{\delta}{2}\right) \sin\left(\frac{\delta}{2}\right) \tag{12}$$

$$Q_2 \approx +\frac{A^2}{\sqrt{r_{12}^{\,2} + x_{12}^{\,2}}} \cos\left(\phi - \frac{\delta}{2}\right) \sin\left(\frac{\delta}{2}\right) \tag{13}$$

The active and reactive powers depend on the voltage amplitude (*A*), phase angle (δ) and line impedance.

Considering inductive lines (i.e., $\Phi \approx 90^o$) line resistances can be neglected, hence the active power will be found to be (14). Furthermore, for resistive lines with small inductances and $\Phi \approx 0^o$, the reactive power can be simplified as (15).

$$\phi \approx 90^o \Rightarrow P_1 \approx +\frac{1}{2}\frac{A^2}{x_{12}} sin(\delta); P_2 \approx -\frac{1}{2}\frac{A^2}{x_{12}} sin(\delta) \tag{14}$$

$$\phi \approx 0^o \Rightarrow Q_1 \approx -\frac{1}{2}\frac{A^2}{r_{12}}\sin(\delta); Q_2 \approx +\frac{1}{2}\frac{A^2}{r_{12}}\sin(\delta) \quad (15)$$

C. Proposed Frequency Droop Approach

Following previous section, depending on the line impedance either active power, reactive power or both play a major role for achieving power sharing among different DC sources. In high *X/R* ratio power systems, according to (14), the active power is associated with the frequency ω, where $\delta = \omega t$. Thereby, in such a systems, the active power can be adjusted by the frequency. While, according to (15), the reactive power can be adjusted by the frequency in low *X/R* ratio power systems.

Meanwhile, in medium *X/R* ratio systems, active and reactive power should be decoupled with decoupling methods [33]. A decoupling matrix is explained in [34] and virtual impedance based methods are widely studied to reshape the output impedance of the converter [33]. In this paper, a virtual resistor merged by the reactive power coupling is proposed for medium *X/R* ratio systems employing frequency droop control for power sharing.

Fig. 3(b) shows the proposed control scheme. The DC voltage is coupled with the reactive power *Q* for low *X/R* ratio systems as well as with the active power *P* for high *X/R* ratio systems. Moreover, the reactive power *Q* is merged by a virtual resistor R_d for medium *X/R* ratio systems. Furthermore, following Fig. 3(b), the AC equivalent model of the converters will be an AC voltage series connected by the virtual resistor R_d. Therefore, the effective *X/R* ratio of the line *k* can be found as $x_k/(r_k+R_d)$.

D. Small Signal Stability Analysis

In this section small signal stability analysis is provided in order to select suitable control parameters. In practice, the inner voltage and current controllers have fast dynamics, hence the low frequency modes of the system associated with the power sharing control loop is analyzed. According to [19], [20], the dominant poles of the low frequency modes can be found as:

$$s^2 + \omega_c s + \frac{\beta}{\alpha} = 0 \quad (16)$$

where *s* is the Laplace operator. α and β are defined as:

$$\alpha = r_1 r_2 - (r_1 + r_2) R_0 \quad (17)$$

$$\beta = 2\pi\omega_c k_\delta d_{f1} d_p \left(r_1\xi + r_2 - 2R_0(\xi + 1)\right) \quad (18)$$

in which ω_c is the cut-off frequency of $G(s) = \omega_c/(s+\omega_c)$, and R_0 is the load resistance at an operating voltage V_{PCC0} and $R_0 = P_{load}/V_{PCC0}$. Furthermore, ξ is as (19) where $I_{r,1}$ and $I_{r,2}$ are the rated currents of converters.

$$\xi = \frac{I_{r,1}}{I_{r,2}} = \frac{d_{f2}}{d_{f1}} \quad (19)$$

k_δ in (18) is obtained by linearizing (14) and (15) as:

$$k_\delta = \begin{cases} \frac{1}{2}\frac{A^2}{x_{12}}\cos(\delta_0) & : high\ X/R \\ \frac{1}{2}\frac{A^2}{r_{12}+2R_d}\cos(\delta_0) & : medium\ X/R \\ \frac{1}{2}\frac{A^2}{r_{12}}\cos(\delta_0) & : low\ X/R \end{cases} \quad (20)$$

where δ_0 is the relative phase angle of superimposed AC

TABLE I. IMPLEMENTED SYSTEM SPECIFICATIONS

Parameter		Symbol	Value
Superimposed frequency		f^* *(Hz)*	50
Superimposed AC voltage		*A (V)*	2.5
Droop gains		d_{f1}, d_{f2} *(Hz/A)*	0.6, 0.3
Power coupling gains		d_q *(V/VA)*	25, 10 (Case III)
DC voltage		V_{DC} *(V)*	400
Inner controllers		Voltage controller $K_{pv}+K_{iv}/s$	0.45 + 20 /*s*
		Current controller $K_{pi}+K_{ii}/s$	0.05 + 2/*s*
Loads		P_{load} *(kW)*	1.2, 0.6
Converter		L_{DC} *(mH)*	2
		C_{DC} *(μF)*	500
		Input /output voltage (V)	300, 400
		Switching Frequency *(kHz)*	20
Line Impedances	Case I	r_1+jx_1 *(Ω)*	0.2 + j0.032
		r_2+jx_2 *(Ω)*	0.2 + j0.032
	Case II	r_1+jx_1 *(Ω)*	0.2 + j0.2
		r_2+jx_2 *(Ω)*	0.2 + j0.2
	Case III	r_1+jx_1 *(Ω)*	0.1 + j0.4
		r_2+jx_2 *(Ω)*	0.1 + j0.4

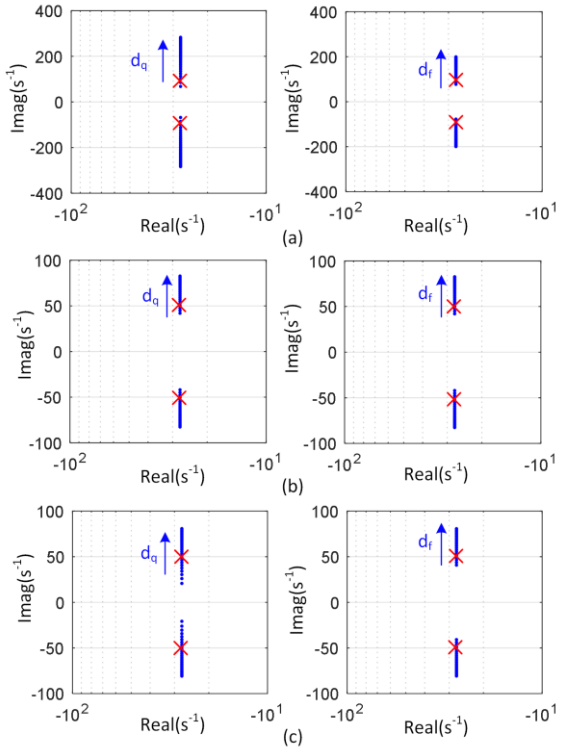

Fig. 7. Effect of d_q and d_f on the dominant poles of the system considering: (a) high *X/R*, (b) medium *X/R* and (c) low *X/R* ratios.

voltages at operating point. Fig. 7 shows the dominant poles places of the system with the given parameters in Table I. The desired poles of the system to have a damping ratio of 0.5 are shown with red (×).

III. Simulation Results

In this section, three simulation cases are provided in order to show the performance of the proposed power management scheme. Furthermore, the performance of the proposed scheme is compared to the conventional droop method. The simulated system includes two boost converters connected to a load as shown in Fig. 2 . The system parameters and line impedances are summarized in Table I. During the simulations, the load is increased from 1.2 *kW* to 1.8 *kW* at $t = 2$ *s*.

A. Case I: Low X/R Ratio Power Grid

In Case I, the feeders of the system are considered to be mostly resistive, which is a reasonable assumption for low voltage power systems. The *X/R* ratio of 0.16 is selected as given in Table I. Therefore, the reactive power is utilized for power sharing control. The simulation results including output voltage and current of the converters as well as the superimposed frequencies are shown in Fig. 8. Following Fig. 8(a), the DC voltages are settled close to the rated value (i.e., 400 *V*). Furthermore, the load current is proportionally supplied by the two converters as shown in Fig. 8(b).

According to the results shown in Fig. 8, employing the reactive power for low *X*/*R* ratio lines causes a proper voltage regulation and load sharing in the grid. Moreover, the proposed frequency-based droop method properly controls the load sharing as the frequency drop is proportional to the output current of each converter. For instance, the first converter current at $t = 2.5$ *s* (blue line in Fig. 8) is 1.5 *A*, hence the frequency should be $50 - 0.6 \times 1.5 = 49.1$ *Hz*, which is obtained by simulations as shown in Fig. 8(c).

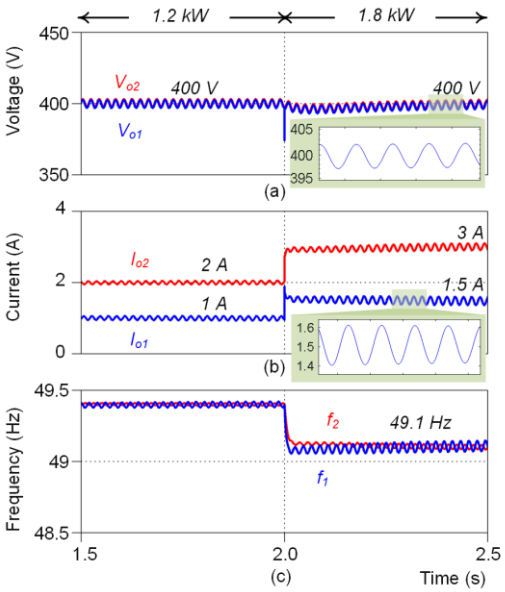

Fig. 8. Obtained simulated results for two converter-based DC grid, considering low *X/R* = 0.16 (i.e., Case I in Table I), controlled by reactive power: (a) DC voltage waveforms, (b) DC current waveforms, and (c) superimposed frequency of both converters.

B. Case II: Medium X/R Ratio Power Grid

In this Case, a medium *X/R* ratio system is simulated with *X*=*R*, and the results are shown in Fig. 9. The reactive power is merged by a virtual resistor equal to 1 Ω is used to reach an appropriate power management in the grid. Therefore, the effective *X/R* ratio, from the AC signals point of view, is 0.2/1.2 = 0.17 and 0.1/1.1 = 0.091 indicating almost resistive lines. As shown in Fig. 9, the converter voltages are adjusted

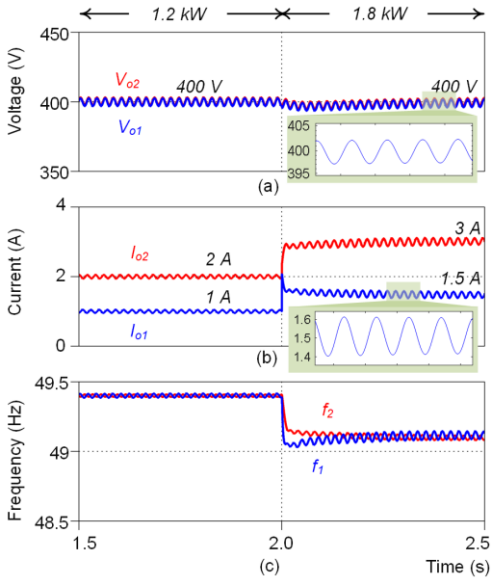

Fig. 9. Obtained simulated results for two converter-based DC grid, with $X \approx R$, controlled by reactive power and virtual resistor (i.e., Case II in Table I): (a) DC voltage waveforms, (b) DC current waveforms, and (c) superimposed frequency of both converters.

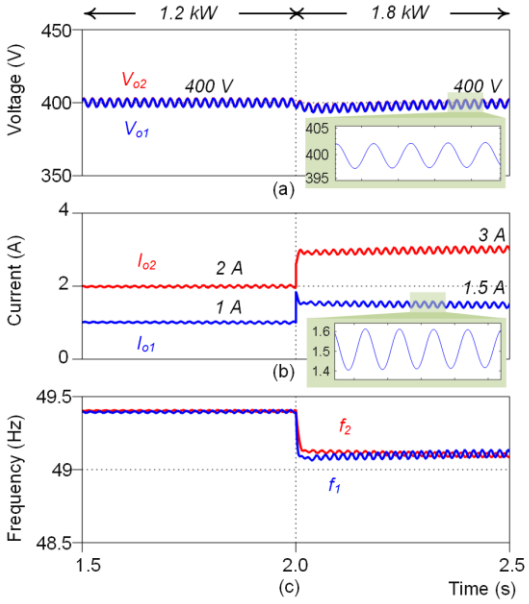

Fig. 10. Obtained simulated results for two converter-based DC grid, considering high *X/R* = 4, controlled by active power (i.e., Case III in Table I): (a) DC voltage waveforms, (b) DC current waveforms, and (c) superimposed frequency of both converters.

close to the rated value and the load current is properly supplied by the two converters as shown in Fig. 9(b). Therefore, in the case of medium voltage power grids with inductive-resistive lines, the reactive power-based frequency droop with a virtual resistor provides a proper power management in the grid. Furthermore, as shown in Fig. 9(c), the injected frequencies are properly converging in steady state and follow the load variation based on the droop gains.

C. Case III: High X/R Ratio Power Grid

In high voltage power systems, the lines are naturally inductive, e.g., *X/R* > 3.3 [33]. Therefore, the active power is suitable for implementing a frequency droop-based power management among DC sources. Fig. 10 shows the voltage, current and frequency waveforms of the converters operating in a high *X/R* ratio DC grid as it is shown in Fig. 10, a proper voltage regulation as well as an accurate current sharing is achieved by the proposed power sharing approach. The frequency variation in terms of load changes is further validating the effectiveness of the proposed scheme for high *X/R* ratio power systems as it is seen in Fig. 10(c).

D. Conventional Droop Control

In order to compare the performance of the frequency droop scheme with conventional droop control [19], the load sharing between the two converters is shown in Fig. 11. The line parameters are given in Table I and line resistances equal to 0.2 Ω. Two simulations are performed with low droop gains, i.e., 2 and 1 Ω for the first and second converters as well as high droop gains equal to 10 and 5 Ω. As shown in Fig. 11(a), with low droop gains, the voltage regulation is (400-396)/400 = 1%, employing the high droop gain introduces (400-385)/400 = 3.75% voltage regulation. Notably, increasing the load causes much voltage drops. However, the sharing ratio between the converters is 2.91/1.59= 1.83 and 2.98/1.52 = 1.96 for low and high droop gains respectively as shown in Fig. 11(b). Therefore, increasing droop gain improves load sharing accuracy while worsen the voltage regulation. This issue will further become important if converters are connected through long lines with large line impedances [35], and hence, extra communication infrastructures are required to fulfill the power management objectives [7]. However, the frequency droop approach offers suitable power sharing and voltage regulation for DC grids without utilizing any communication networks proposing a reliable and cost-effective solution.

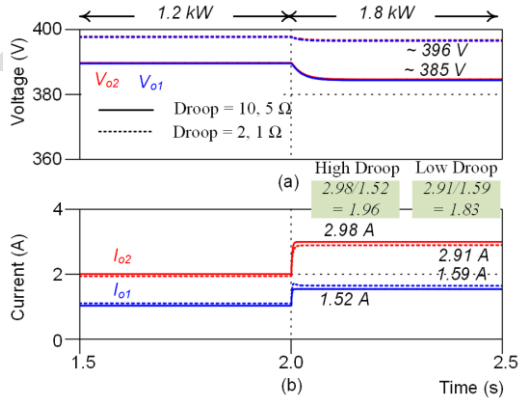

Fig. 11. Obtained simulated results utilizing conventional droop method for two converter-based DC grid, with line impedances of Case I: (a) DC voltage, (b) DC current waveforms.

IV. Experimental Results

To further evaluate the viability of the proposed control strategies, two DC/DC boost converters are implemented as shown in Fig. 12, where each converter is controlled by an individual Digital Signal Processor (DSP: TMS320F28335). In order to model the lines with different *X/R* ratios in a scaled-down prototype, suitable combination of series-connected inductor and resistor are selected as summarized in Table I.

The experimental results shown in Fig. 13 to Fig. 15 demonstrates the performance of the proposed load sharing approach. During the tests, the load is changed from 1.2 *kW* to 1.8 *kW*. For a low voltage system, the *X/R* ratio is selected to be 0.16, and the results are shown in Fig. 13. As it is shown in Fig. 13, utilizing the reactive power results in appropriate voltage regulation and load sharing between the converters. This approach is also presented in [19]. Moreover. the merged reactive-power based droop and virtual resistor is utilized for medium *X/R* ratio equal to 1. Hence, the voltages are adjusted close to the rated value and the load power is accurately shares between the sources as shown in Fig. 14. Finally, the performance of applying the active power to the AC to DC coupling stage for the high *X/R* = 4 is shown in Fig. 15.

Obtained experimental results reported in Fig. 13 to Fig. 15 implies the effectiveness of the frequency droop based power sharing method for DC grids at different *X/R* ratios. This approach introduces a decentralized power management among DC sources without utilizing a physical communication network, while providing an appropriate voltage regulation.

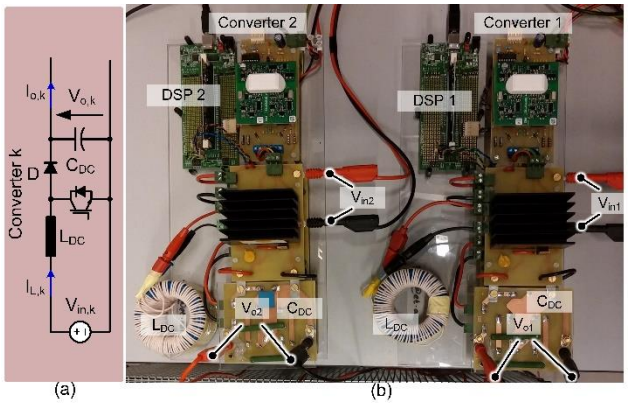

Fig. 12. Implemented two-converter/based microgrid; (a) schematic of boost converter, and (b) implemented prototypes.

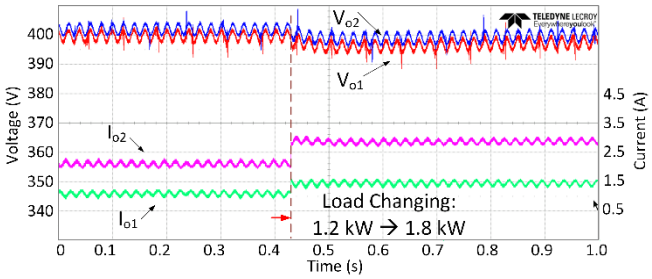

Fig. 13. Measured experimental result for a DC grid with low X/R = 0.16.

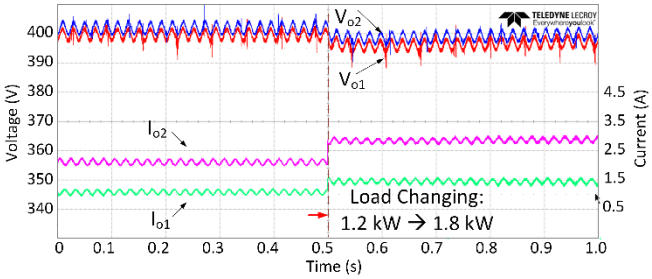

Fig. 14. Measured experimental result for a DC grid with medium X/R = 1.

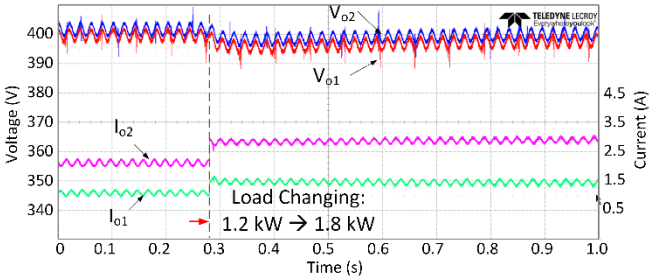

Fig. 15. Measured experimental result for a DC grid with high X/R = 4.

V. PERSPECTIVES

Signal injection approaches are employed for protection, islanding detection, and identification in power systems, where signal injection is performed periodically for a short time. In the power sharing application, the proposed frequency injection method can be used to determine the suitable droop gains according to the operating point. Furthermore, this approach can be applied for multi-connected converters in DC grids. As a consequence, the overall system efficiency and power quality will not be affected by the signal injection approach. In the following, a simulation case study is provided demonstrating applicability of the proposed event-triggered limited-time signal injection approach in a five-bus system with three converters as shown in Fig. 16.

The obtained simulation results are depicted in Fig. 16, which two 2 kW loads are supplied equally by the three units following the frequency-droop scheme. Notably, here the limited-time signal injection strategy is applied as at t = 2 s the

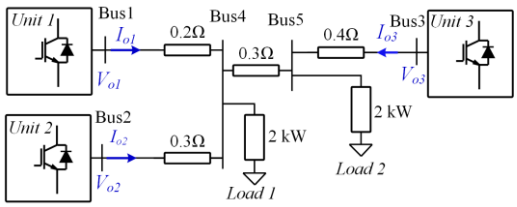

Fig. 16. DC grid with three units and two loads.

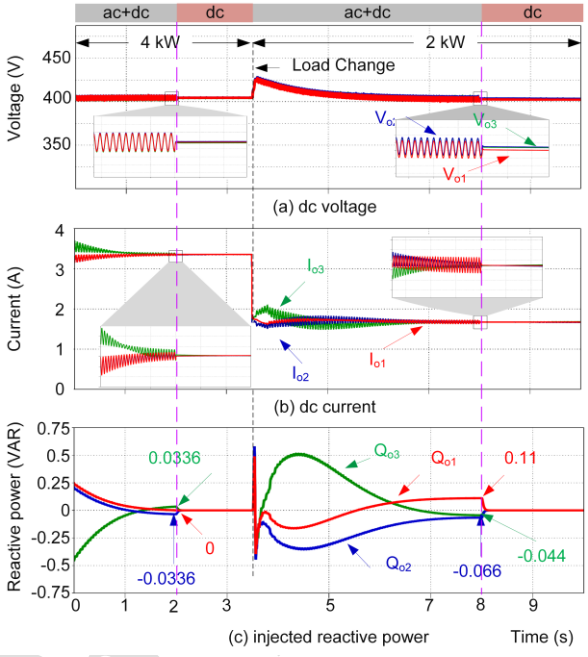

Fig. 17. Simulation results of the limited-time signal injection approach for multi-connected converters with X/R = 0.16, (a) voltages, (b) currents, and (c) injected reactive power of converters.

controller stops the signal injection as soon as the output voltage reaches its steady-state value. Furthermore, since the system is operating under low X/R ratio and the AC signal injection is stopped, the control system utilizes the injected reactive powers before stopping signal injection to maintain the power sharing performance during a pure DC operation mode. These values are equal to 0, -0.0336 and +0.0366 VAR as shown in Fig. 17(c). At t = 3.5 s, $Load_1$ on bus 4 is disconnected.

Thereby, the signal injection is started to achieve suitable load sharing and voltage regulation among the units as shown in Fig. 17(a, b). At t = 8 s, the signal injection is stopped and the control system takes the last values of the reactive power of 0.11, 0.066, and 0.044 VAR respectively for first, second and third units as shown in Fig. 17(c). These reactive powers are not the same as the ones for supplying both loads. Because the effective line resistors, for two cases are different following the grid topology shown in Fig. 16. Therefore, the proposed control strategy is adaptable to different DC grid architectures.

VI. Further Evaluation

The viability of the proposed control strategy is further evaluated considering the unequal loading of converters in a multi-converter system with a 10 kW load (Load 1 = 5 kW and Load 2 = 5 kW in Fig. 16). The rated power of third converter is half of the others. The simulation results are shown in Fig. 18. At first, the converters 1 and 2 are supplying the load with equal current of 12.5 A as shown in Fig. 18(b). The third converter is connected at t = 0.5 s. As it can be seen in this figure, the output current of third converter is 5 A and the other converters are equally supplying 10 A. Therefore, the load sharing is properly performed and the voltages are regulated close to the rated value as shown in Fig. 18(a).

VII. Conclusion

A decentralized frequency-based droop scheme is addressed in this paper for DC grid systems applicable to high/medium/low voltage DC power systems. The control approach includes two merged AC and DC droop characteristics, i.e., frequency-current droop and voltage-power droop controllers. The proposed approach couples the DC voltage to the reactive power, which results in an appropriate load sharing in low voltage power grid (i.e., low *X/R* ratio), while coupling the DC voltage to the active power is appropriate for power systems with high *X/R* ratio. Meanwhile, coupling a DC voltage with the reactive power merged to the virtual resistor brings a suitable load sharing for power systems medium low *X/R* ratio. Furthermore, utilizing superimposed AC voltage significantly improve voltage regulation in DC grids due to preventing the use of conventional droop resistors. The proposed approach can be further developed to improve its performance and efficiency by stopping the signal injection in steady state after determining a suitable droop gains following an operation condition. The obtained simulation and experimental results show a closed agreement with the provided analytical analysis and validates the performance of the proposed frequency injection scheme under different *X/R* ratios.

References

[1] J. G. Ciezki and R. W. Ashton, "Selection and Stability Issues Associated with a Navy Shipboard DC Zonal Electric Distribution System," *IEEE Trans. Power Deliv.*, vol. 15, no. 2, pp. 665–669, Apr. 2000.

[2] D. Boroyevich, I. Cvetkovic, R. Burgos, and D. Dong, "Intergrid: A Future Electronic Energy Network?," *IEEE J. Emerg. Sel. Top. Power Electron.*, vol. 1, no. 3, pp. 127–138, 2013.

[3] P. Kou, D. Liang, J. Wang, and L. Gao, "Stable and Optimal Load Sharing of Multiple PMSGs in an Islanded DC Microgrid," *IEEE Trans. Energy Convers.*, vol. 33, no. 1, pp. 260–271, Mar. 2018.

[4] M. R. Hossain and H. L. Ginn, "Real-Time Distributed Coordination of Power Electronic Converters in a DC Shipboard Distribution System," *IEEE Trans. Energy Convers.*, vol. 32, no. 2, pp. 770–778, Jun. 2017.

[5] S. Peyghami-Akhuleh, H. Mokhtari, P. Davari, P. C. Loh, and F. Blaabjerg, "Smart Power Management of DC Microgrids in Future Milligrids," in *Proc. IEEE EPE*, 2016, pp. 1–10.

[6] J. M. Guerrero, J. C. Vasquez, J. Matas, L. G. De Vicuña, and M. Castilla, "Hierarchical Control of Droop-Controlled AC and DC Microgrids - A General Approach toward Standardization," *IEEE Trans. Ind. Electron.*, vol. 58, no. 1, pp. 158–172, 2011.

[7] V. Nasirian, A. Davoudi, F. L. Lewis, and J. M. Guerrero, "Distributed Adaptive Droop Control for Dc Distribution Systems," *IEEE Trans. Energy Convers.*, vol. 29, no. 4, pp. 944–956, 2014.

[8] S. Anand, B. G. Fernandes, and J. M. Guerrero, "Distributed Control to Ensure Proportional Load Sharing and Improve Voltage Regulation in Low-Voltage DC Microgrids," *IEEE Trans. Power Electron.*, vol. 28, no. 4, pp. 1900–1913, 2013.

[9] A. Khorsandi, M. Ashourloo, and H. Mokhtari, "A Decentralized Control Method for a Low-Voltage DC Microgrid," *IEEE Trans. Energy Convers.*, vol. 29, no. 4, pp. 793–801, 2014.

[10] X. Lu, J. M. Guerrero, K. Sun, and J. C. Vasquez, "An Improved Droop Control Method for DC Microgrids Based on Low Bandwidth Communication With DC Bus Voltage Restoration and Enhanced Current Sharing Accuracy," *IEEE Trans. Power Electron.*, vol. 29, no. 4, pp. 1800–1812, Apr. 2014.

[11] Y. Gu, X. Xiang, W. Li, and X. He, "Mode-Adaptive Decentralized Control for Renewable DC Microgrid With Enhanced Reliability and Flexibility," *IEEE Trans. Power Electron.*, vol. 29, no. 9, pp. 5072–5080, 2014.

[12] T. Dragicevic, J. M. Guerrero, J. C. Vasquez, and D. Skrlec, "Supervisory Control of an Adaptive-Droop Regulated DC Microgrid with Battery Management Capability," *IEEE Trans. Power Electron.*, vol. 29, no. 2, pp. 695–706, 2014.

[13] P.-H. Huang, P.-C. Liu, W. Xiao, and M. S. El Moursi, "A Novel Droop-Based Average Voltage Sharing Control Strategy for DC Microgrids," *IEEE Trans. Smart Grid*, vol. 6, no. 3, pp. 1096–1106, May 2015.

[14] T.-F. Wu, Y.-K. Chen, and Y.-H. Huang, "3C Strategy for Inverters in Parallel Operation Achieving an Equal Current Distribution," *IEEE Trans. Ind. Electron.*, vol. 47, no. 2, pp. 273–281, Apr. 2000.

[15] J. M. Guerrero, L. Hang, and J. Uceda, "Control of Distributed Uninterruptible Power Supply Systems," *IEEE Trans. Ind. Electron.*, vol. 55, no. 8, pp. 2845–2859, 2008.

[16] A. Khorsandi, M. Ashourloo, H. Mokhtari, and R. Iravani, "Automatic Droop Control for a Low Voltage DC Microgrid," *IET Gener. Transm. Distrib.*, vol. 10, no. 1, pp. 41–47, Jan. 2016.

[17] D. Perreault, R. Selders, and J. Kassakian, "Frequency-Based Current-Sharing Techniques for Paralleled Power Converters," *IEEE Trans. Power Electron.*, vol. 13, no. 4, pp. 626–634, 1998.

[18] A. Tuladhar and H. Jin, "A Novel Control Technique to Operate DC/DC Converters in Parallel with No Control Interconnections," in *Proc. IEEE PESC*, 1998, vol. 1, pp. 892–898.

[19] S. Peyghami, P. Davari, H. Mokhtari, P. C. Loh, and F. Blaabjerg, "Synchronverter-Enabled DC Power Sharing Approach for LVDC Microgrids," *IEEE Trans. Power Electron.*, vol. 32, no. 10, pp. 8089–8099, Oct. 2017.

[20] S. Peyghami, H. Mokhtari, P. C. Loh, P. Davari, and F. Blaabjerg, "Distributed Primary and Secondary Power Sharing in a Droop-Controlled LVDC Microgrid with Merged AC and DC

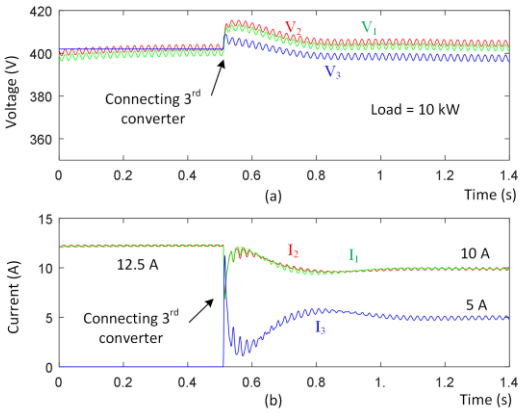

Fig. 18. Simulation results of unequal load sharing with synchronization of the third converter at t = 0.5 *s*; (a) voltages, (b) currents – *X/R* = 0.16.

Characteristics," *IEEE Trans. Smart Grid*, vol. 9, no. 3, pp. 2284–2294, 2018.
[21] F. Mura and R. W. De Doncker, "Design Aspects of a Medium-Voltage Direct Current (MVDC) Grid for a University Campus," in *Proc. IEEE ECCE*, 2011, pp. 2359–2366.
[22] U. Javaid, D. Dujic, and W. van der Merwe, "MVDC Marine Electrical Distribution: Are We Ready?," in *Proc. IEEE IECON*, 2015, pp. 000823–000828.
[23] M. Cupelli, M. Mirz, and A. Monti, "Application of Backstepping to MVDC Ship Power Systems with Constant Power Loads," in *Proc. IEEE ESARS*, 2015, pp. 1–6.
[24] G. F. Reed, B. M. Grainger, A. R. Sparacino, R. J. Kerestes, and M. J. Korytowski, "Advancements in Medium Voltage DC Architecture Development with Applications for Powering Electric Vehicle Charging Stations," in *Proc. IEEE Energytech*, 2012, pp. 1–8.
[25] G. Lambert, M. V. Soares, P. Wheeler, M. L. Heldwein, and Y. R. de Novaes, "Current Fed Multipulse Rectifier Approach for Unidirectional HVDC and MVDC Applications," *IEEE Trans. Power Electron.*, p. Early Access, 2018.
[26] Y. Khersonsky, T. Ericsen, P. Bishop, J. Amy, M. Andrus, T. Baldwin, B. Bartolucci, N. Benavides, D. Boroyevich, A. Chaudhary, and D. Clayton, "IEEE Recommended Practice for 1 KV to 35 KV Medium-Voltage DC Power Systems on Ships," Institute of Electrical and Electronics Engineers (IEEE), 2010.
[27] A. R. . Z.-H. M. Reed, G.F.; Grainger, B.M.; Sparacino, "Ship to Grid: Medium-Voltage DC Concepts in Theory and Practice," *IEEE Power Energy Mag.*, vol. 10, no. 6, pp. 70–79, 2012.
[28] E. Alliance, "380 Vdc Architectures for the Modern Data Center," 2013. [Online]. Available: http://www.emergealliance.org/. [Accessed: 01-Jan-2016].
[29] B. T. Patterson, "DC, Come Home: DC Microgrids and the Birth of the 'Enernet,'" *IEEE Power Energy Mag.*, vol. 10, no. 6, pp. 60–69, 2012.
[30] D. Salomonsson, S. Member, L. Söder, and A. Sannino, "An Adaptive Control System for a DC Microgrid for Data Centers," *IEEE Trans. Ind. Appl.*, vol. 44, no. 6, pp. 1910–1917, 2008.
[31] Y. Yang, Y. Qin, S. C. Tan, and R. Hui, "Efficient Improvement of Photovoltaic-Battery Systems in Standalone DC Microgrids Using A Local Hierarchical Control for the Battery System," *IEEE Trans. Power Electron.*, vol. 99, no. 10.1109/TPEL.2019.2900147, pp. 1–11, 2019.
[32] D. Shi, X. Chen, Z. Wang, X. Zhang, Z. Yu, X. Wang, and D. Bian, "A Distributed Cooperative Control Framework for Synchronized Reconnection of a Multi-Bus Microgrid," *IEEE Trans. Smart Grid*, vol. 9, no. 6, pp. 6646–6655, Nov. 2018.
[33] J. Rocabert, A. Luna, F. Blaabjerg, and P. Rodriguez, "Control of Power Converters in AC Microgrids," *IEEE Trans. Power Electron.*, vol. 27, no. 11, pp. 4734–4749, 2012.
[34] M. Karimi-Ghartemani, "Universal Integrated Synchronization and Control for Single-Phase DC/AC Converters," *IEEE Trans. Power Electron.*, vol. 30, no. 3, pp. 1544–1557, 2015.
[35] S. Peyghami, H. Mokhtari, P. Davari, P. C. Loh, and F. Blaabjerg, "On Secondary Control Approaches for Voltage Regulation in DC Microgrids," *IEEE Trans. Ind. Appl.*, vol. 53, no. 5, pp. 4855–4862, Sep. 2017.

Saeed Peyghami, (S'14–M'17) was born in Tabriz, Iran on 1988. He received the B.Sc., M.Sc. and Ph.D. degrees all in electrical engineering, power electronics from the Department of Electrical Engineering, Sharif University of Technology, Tehran, Iran, in 2010, 2012, 2017 respectively. He was a Visiting Ph.D. Scholar with the Department of Energy Technology, Aalborg University, Denmark in 2015 to 2016, where he is currently a Postdoctoral researcher. His research interests include power electronics, microgrids, renewable energies, and reliability.

Pooya Davari (S'11–M'13-SM'19) received the B.Sc. and M.Sc. degrees in electronic engineering from the University of Mazandaran, Babolsar, Iran, in 2004 and 2008, respectively, and the Ph.D. degree in power electronics from Queensland University of Technology (QUT), Brisbane, Australia, in 2013. From 2005 to 2010, he was involved in several electronics and power electronics projects as a Development Engineer. From 2010 to 2014, he investigated and developed high-power high-voltage power electronic systems for multidisciplinary projects, such as ultrasound application, exhaust gas emission reduction, and tissue-materials sterilization. From 2013 to 2014, he was a Lecturer with QUT. He joined as a Postdoctoral Researcher the Department of Energy Technology, Aalborg University, Aalborg, Denmark, in 2014, where he is currently an Associate Professor. His current research interests include EMI/EMC in power electronics, WBG-based power converters, active front-end rectifiers, harmonic mitigation in adjustable-speed drives, and pulsed power applications. Dr. Davari received a research grant from the Danish Council of Independent Research in 2016.

Hossein Mokhtari (M'03–SM'14) was born in Tehran, Iran, on August 19, 1966. He received the B.Sc. degree in electrical engineering from Tehran University, Tehran, in 1989. He received the M.Sc. degree in power electronics from the University of New Brunswick, Fredericton, NB, Canada, in 1994, and the Ph.D. degree in power electronics/power quality from the University of Toronto, Toronto, ON, Canada in 1999.

From 1989 to 1992, he worked in the Consulting Division of Power Systems Dispatching Projects, Electric Power Research Center Institute, Tehran. Since 2000, he has been with the Department of Electrical Engineering, Sharif University of Technology, Tehran, where he is currently a Professor. He is also a Senior Consultant to several utilities and industries.

Frede Blaabjerg (S'86–M'88–SM'97–F'03) was with ABB-Scandia, Randers, Denmark, from 1987 to 1988. From 1988 to 1992, he got the PhD degree in Electrical Engineering at Aalborg University in 1995. He became an Assistant Professor in 1992, an Associate Professor in 1996, and a Full Professor of power electronics and drives in 1998. From 2017 he became a Villum Investigator.

He is honoris causa at University Politehnica Timisoara (UPT), Romania and Tallinn Technical University (TTU) in Estonia.

His current research interests include power electronics and its applications such as in wind turbines, PV systems, reliability, harmonics and adjustable speed drives. He has published more than 600 journal papers in the fields of power electronics and its applications. He is the co-author of four monographs and editor of ten books in power electronics and its applications.

He has received 29 IEEE Prize Paper Awards, the IEEE PELS Distinguished Service Award in 2009, the EPE-PEMC Council Award in 2010, the IEEE William E. Newell Power Electronics Award 2014 and the Villum Kann Rasmussen Research Award 2014. He was the Editor-in-Chief of the IEEE TRANSACTIONS ON POWER ELECTRONICS from 2006 to 2012. He has been Distinguished Lecturer for the IEEE Power Electronics Society from 2005 to 2007 and for the IEEE Industry Applications Society from 2010 to 2011 as well as 2017 to 2018. In 2018 he is President Elect of IEEE Power Electronics Society. He serves as Vice-President of the Danish Academy of Technical Sciences. He is nominated in 2014, 2015, 2016 and 2017 by Thomson Reuters to be between the most 250 cited researchers in Engineering in the world.